

## Supplementary Information

### **A dual underliquid superlyophobic surface in organic media for on-demand separation of immiscible organic liquid mixtures**

Yihan Sun <sup>a,c</sup> Jinxia Huang <sup>a\*</sup>, and Zhiguang Guo <sup>a,b,\*</sup>

<sup>a</sup> State Key Laboratory of Solid Lubrication, Lanzhou Institute of Chemical Physics, Chinese Academy of Sciences, Lanzhou 730000, People's Republic of China

<sup>b</sup> Ministry of Education Key Laboratory for the Green Preparation and Application of Functional Materials, Hubei University, Wuhan 430062, People's Republic of China

<sup>c</sup> University of Chinese Academy of Sciences, Beijing 100049, People's Republic of China

\* Corresponding author.

*E-mail addresses:* [zguo@licp.cas.cn](mailto:zguo@licp.cas.cn) (Z. Guo) and [huangjx@licp.cas.cn](mailto:huangjx@licp.cas.cn) (J. Huang).

## Experiment section

### *Materials.*

Titanium dioxide (TiO<sub>2</sub>, AEROXIDE P25) nanoparticles with an average diameter about 25 nm was purchased from DEGUSSA Co., Ltd., Germany. Silica (SiO<sub>2</sub>) nanoparticle with an average diameter of 15 nm and zirconium dioxide (ZrO<sub>2</sub>) nanoparticle with 50 nm were provided by Meryer Chemical Technology Co., Ltd., and Aladdin Co., Ltd., respectively. Copper sheet, stainless-steel mesh (SSM), nickel foam (NF) and ceramic sheet were commercially available. The used fluorocarbon surfactant Zonyl 9977 was obtained from DuPont Chemical Industry. The used organic solvents including 1,2-dichloroethane (DCE), formamide (FA), iso-octane (IST), dimethyl sulfoxide (DMSO) and petroleum ether (PE) are all of analytical grade, and are all provided by Rionlon Chemical Reagent Co., Ltd. Deionized water was used in the whole experiment section. The dielectric constant and surface tension of the used liquids at 25 °C were obtained from Lange's Handbook of Chemistry and are listed in Table S2 in supporting information.

### *Preparation of the superwetting surfaces.*

1g P25 was dispersed into the 15 ml ethanol-water cosolvent containing a certain weight of Zonyl 9977. The volume of ethanol and water is adjusted to 10 ml and 5 ml, respectively. After mechanically stirred for 30 min, the developed white spraying inks were uniformly sprayed-coated on SSM and other used substrates in a line-to-line fashion using a spraying gun with 0.2 MPa nitrogen gas. The spraying distance between spraying gun's nozzle and substrate was maintained about 20 cm. To remove the residual solvents and strengthen the mechanical robustness of the coating, the spraying-coated surfaces were cured at 120 °C for 1h.

### *The on-demand immiscible organic liquid mixture separation.*

The spraying -coated SSM was fixed between the two glass tubes with an effective separation area of 3.14 cm<sup>2</sup>. The separating system was placed vertically. The immiscible organic liquid mixtures (50%, v/v) were poured onto the coated SSM surface that was prewetted by permeated liquids. The separating flux was calculated by measuring the time after collecting 15 ml permeated liquids. According to the following equation, the separation efficiency was determined by measuring the mass of permeated liquids before and after separation.

$$\text{Separation efficiency (\%)} = m_{\text{after}} / m_{\text{before}} \times 100\%$$

$m_{\text{before}}$  and  $m_{\text{after}}$  represent the mass of permeated liquids before and after separation, respectively.

### *The mechanical robustness and chemical stability test.*

The mechanical robustness of the as-prepared membrane in separation process was evaluated by measuring the maximum height of the stagnated liquid that membrane can support to determine the intrusion pressure. The coated SSM was prewetted by FA, and various immiscible organic liquids were separately poured onto the coated SSM. The maximum height of the blocked liquid layer before permeated through the mesh was measured by a metric ruler. The chemical stability of the

coating was estimated by characterizing its resistance to the corrosion from organic solvents. The underliquid contact angles on SSM that was immersed into various organic solvents were measured after submersion for 5 days.

### ***Characterization.***

All the optical photographs were taken by a cellphone (HUAMEI Mate 9). The surface topography of the samples was observed using an environmental scanning electron microscope (ESEM, FEI QUANTA FEG 650). The accelerating voltage were 30 kv and the samples were sputtered-coated with Au before observation. X-ray spectroscopy (EDS) detector (APEX<sup>TM</sup> Standard) attached to ESEM and X-ray photoelectron spectroscopy (XPS, Thermo Scientific ESCALAB 250Xi) using a Al K $\alpha$  radiation sources were both used to investigate the surface chemical element component of the samples. Fourier transform infrared spectra (FTIR, Thermo Scientific Nicolet iS10) was used to investigate the surface chemical composition of the used nanoparticles. The crystal structures of the samples were studied by measuring X-ray diffraction (XRD) patterns using an XRD diffractometer (X'PERT PRO). The contact angles (CA) and sliding angles (SA) were measured using a JC 20001 contact angle measuring system (Zhongchen Digital Equipment Co., Ltd. Shanghai, China). The average contact angles and sliding angles were obtained by measuring the three different positions at the test samples. All the volume of the test liquid droplets was 5  $\mu$ L. The residual content of the blocked liquid in the collected liquid was measured by a gas chromatography (SHIMADZU, GC-2014C). The average surface roughness was measured using a MicroXAM-800 3D profilometer (KLA-Tencor Corporation, Milpitas, USA), and the average values were obtained by measuring three times at different locations.

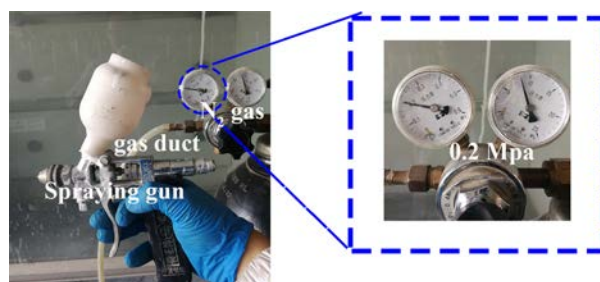


**Figure S1.** The photography of the used spraying coating installment. The spraying suspension was uniformly coated in a line-to-line fashion onto the vertically placed substrates using spraying gun (LOTUS No.1, Shanghai YuGong Hardware Tool Co, Ltd) under the operation of 0.2 MPa N<sub>2</sub> gas. The average diameter of the spraying nozzle is 0.8 mm. The spraying distances between the used spraying gun and substrates are all adjusted to 20 cm.

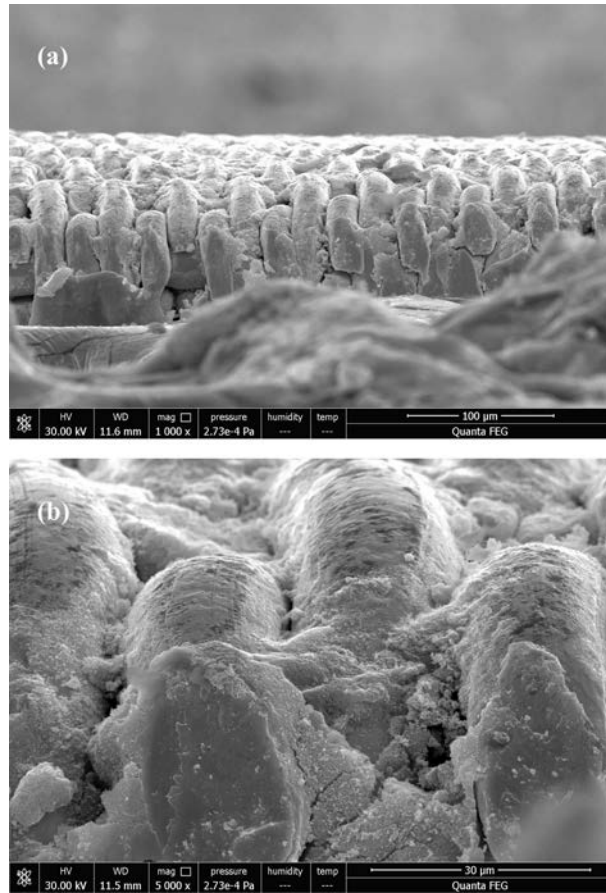


**Figure S2.** The cross-section view of SEM images of the coated SSM. The average thickness of the coating on SSM is about 8μm.

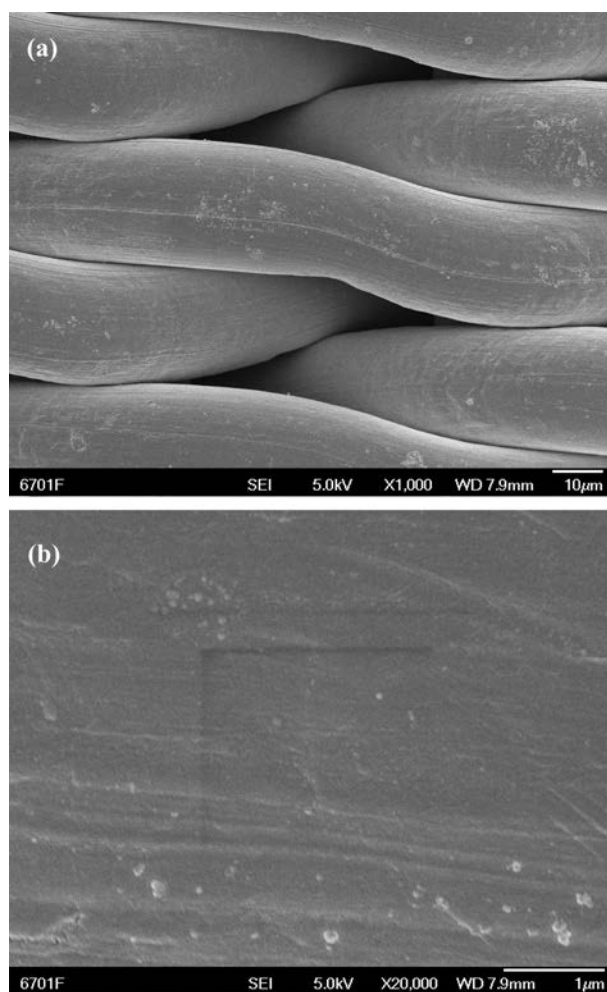


**Figure S3.** The SEM images of the pristine SSM show that the pristine SSM have a smooth surface topography and the average pore size is approximate 5  $\mu\text{m}$ .

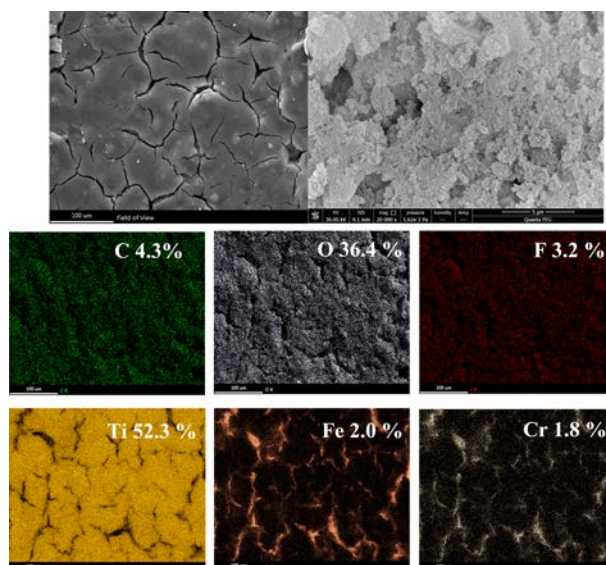


**Figure S4.** ESEM images and EDS mapping of Z(0.5) SSM.

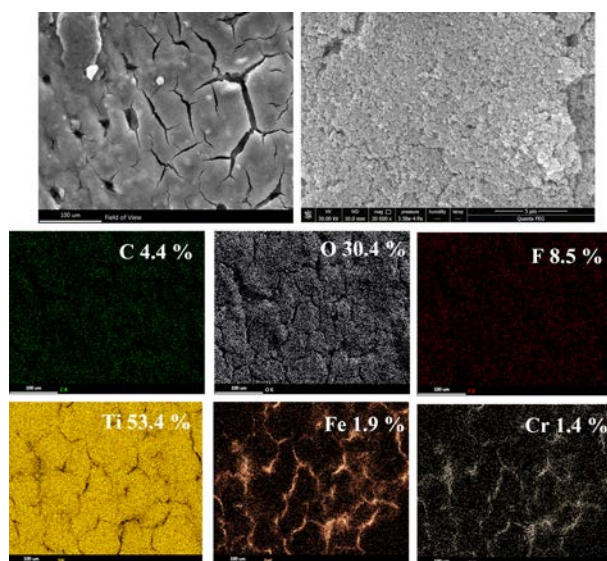


**Figure S5.** ESEM images and EDS mapping of Z(1.0) SSM.



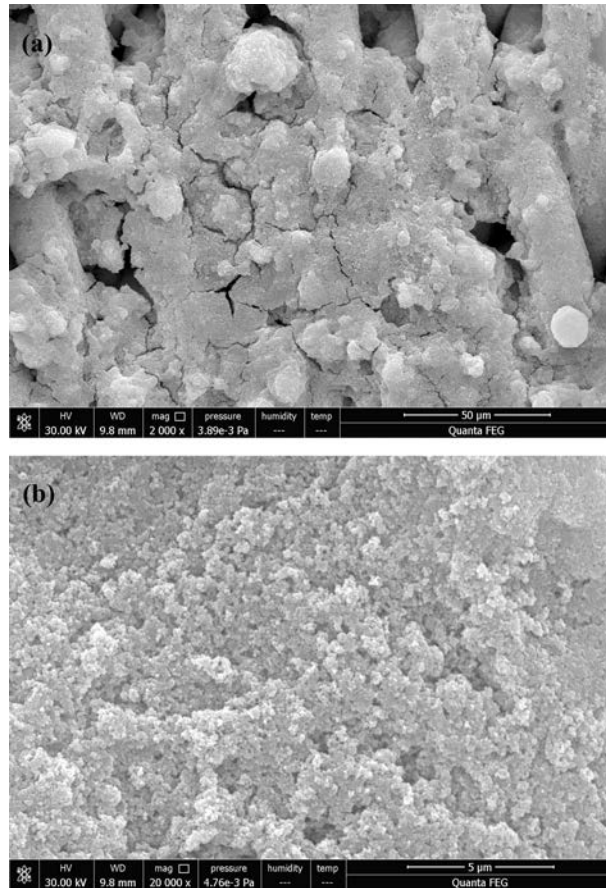


**Figure S6.** The ESEM images of the coated SSM using the coating suspension only containing P25.

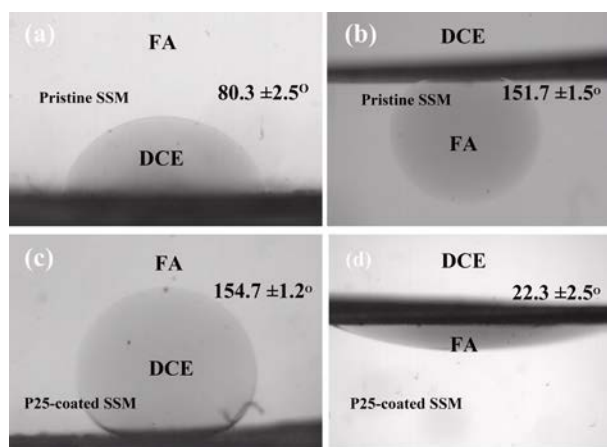


**Figure S7.** The wettability of the pristine SSM and coated SSM using the coating dispersion only containing P25.

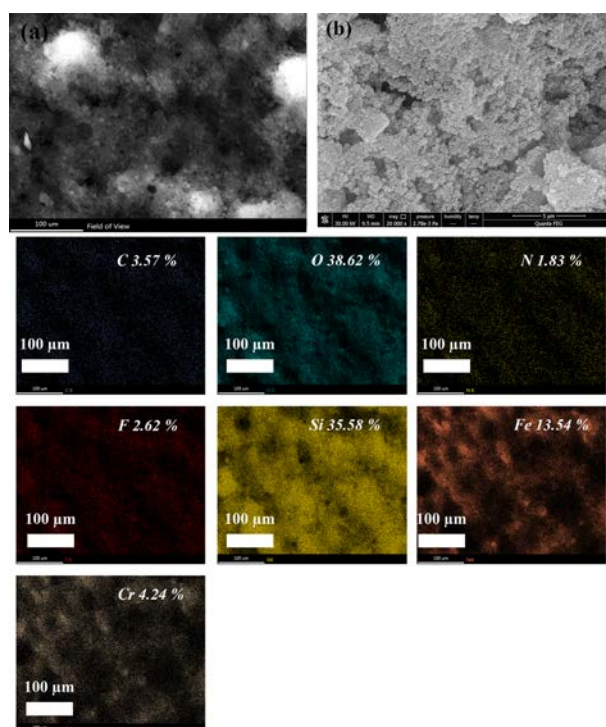


**Figure S8.** The SEM images and EDS mapping of the coated SSM using silica (SiO<sub>2</sub>) nanoparticles

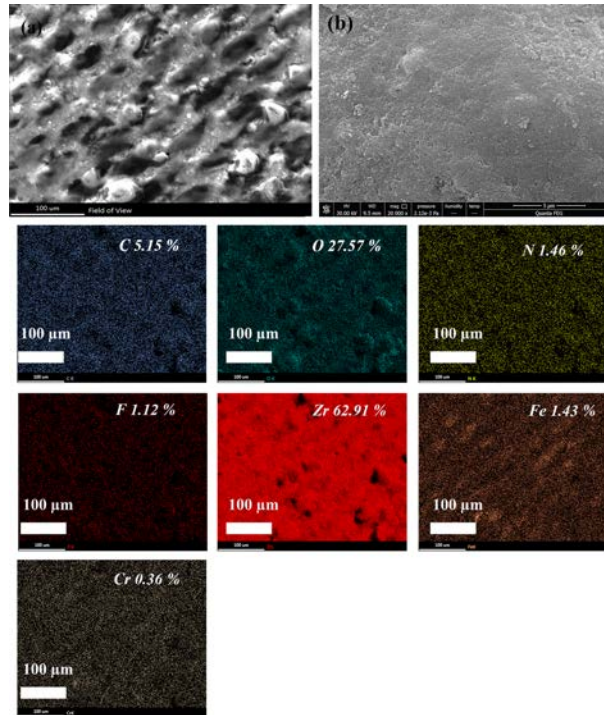


**Figure S9.** The SEM images and EDS mapping of the coated SSM using zirconium dioxide ( $\text{ZrO}_2$ ) nanoparticles.

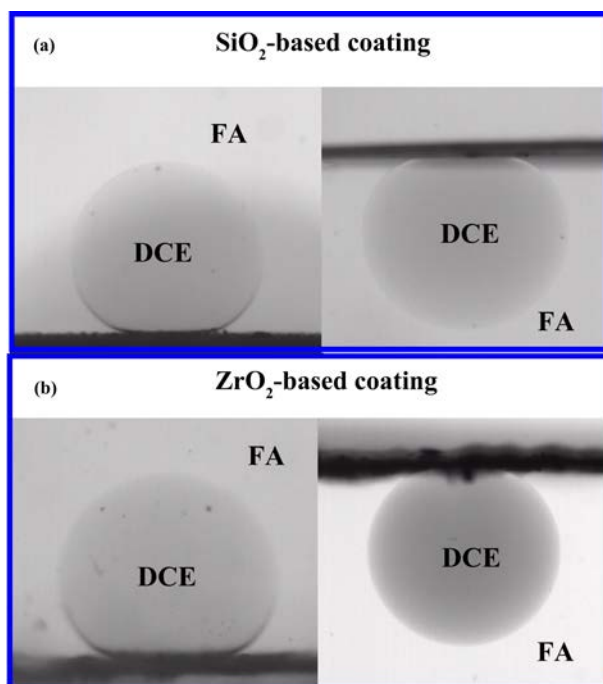


**Figure S10.** The wettability of the coated SSM using SiO<sub>2</sub> and ZrO<sub>2</sub> nanoparticles in opposite organic media.

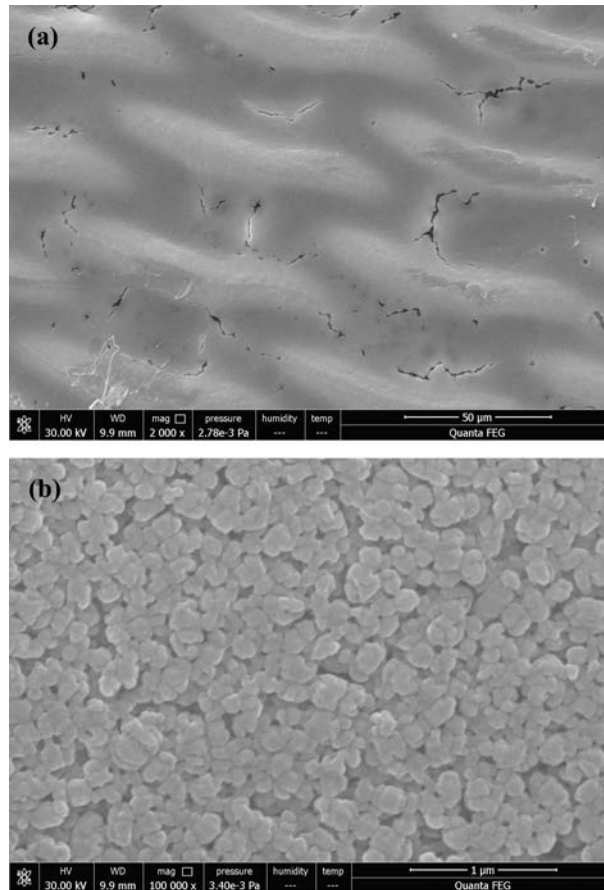


**Figure S11.** The SEM images of the coated SSM using PTFE nanoparticles.

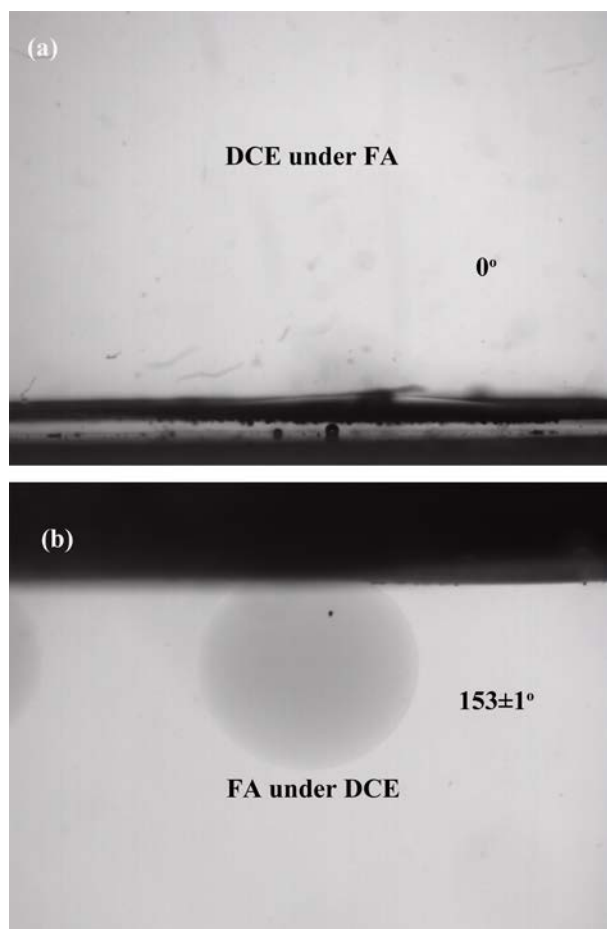


**Figure S12.** The wettability of the coated SSM using PTFE nanoparticles in opposite organic media.

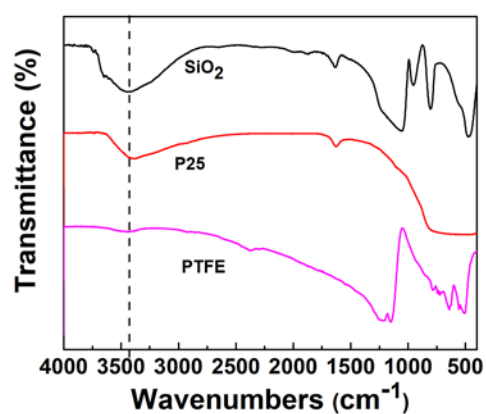


**Figure S13.** The FTIR spectra of the used nanoparticles including  $\text{SiO}_2$ , P25 and PTFE nanoparticles. From the results, it can be observed that the surface of PTFE nanoparticles lacks the peak at about  $3480\text{ cm}^{-1}$  that can be assigned to -OH vibration.



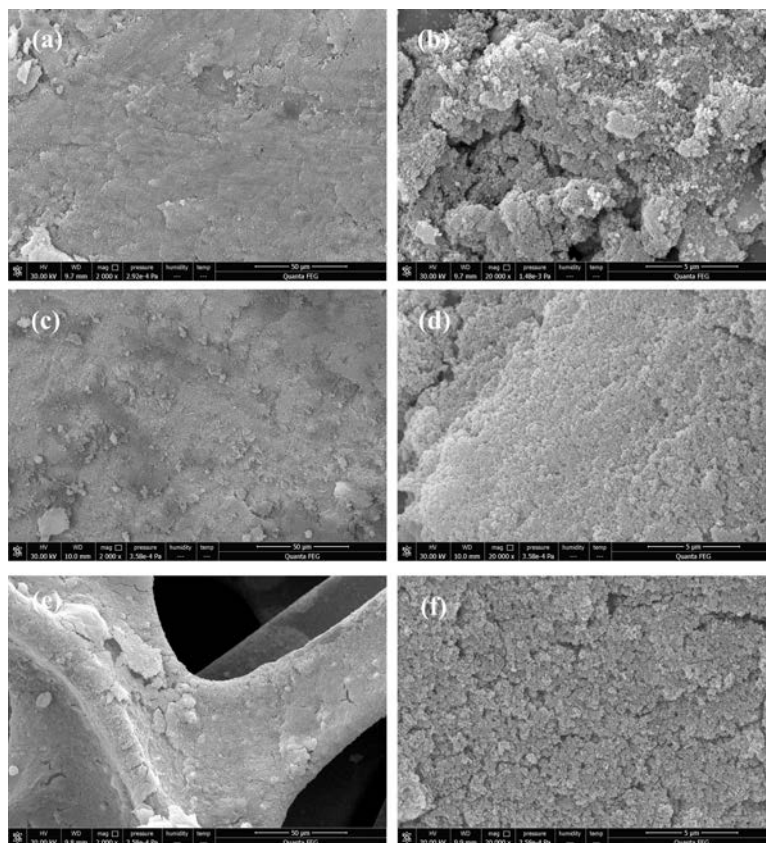


**Figure S14.** The ESEM images of the coated ceramic sheet (a, b), copper sheet (c, d) and nickel foam (e, f).

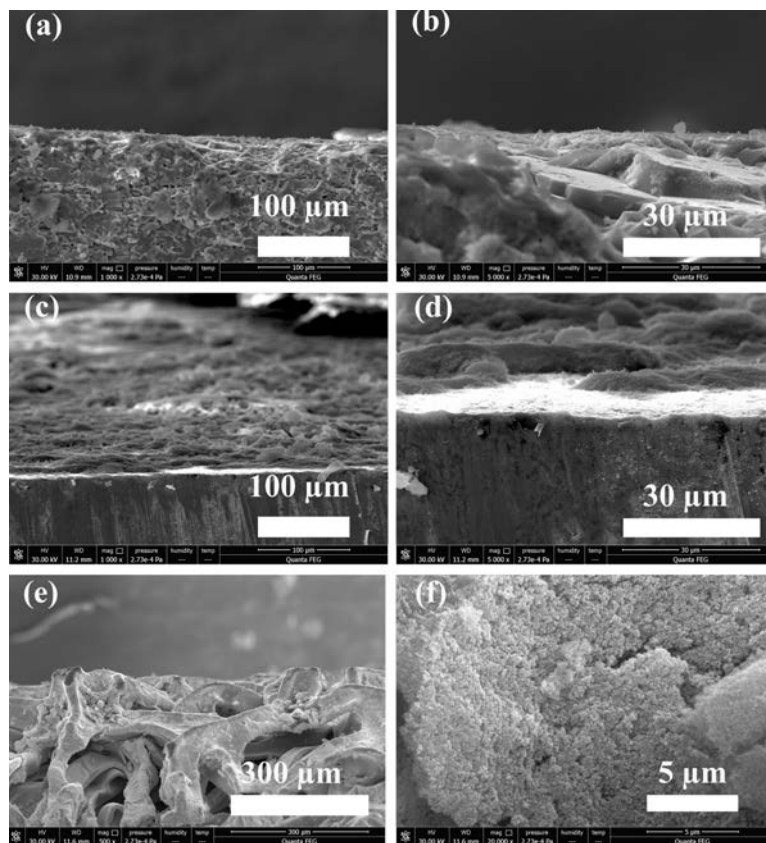


**Figure S15.** The cross-section view of ESEM images of the coated ceramic sheet (a, b), copper sheet (c, d) and nickel foam (e, f).

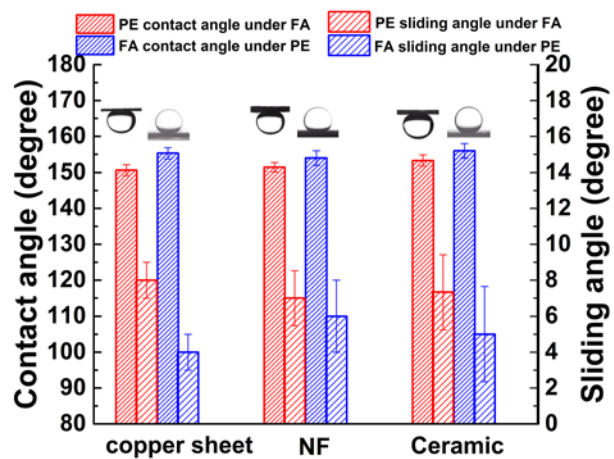


**Figure S16.** The wettability of the coated various substrates including copper sheet, ceramic and nickel foam in the opposite organic media.

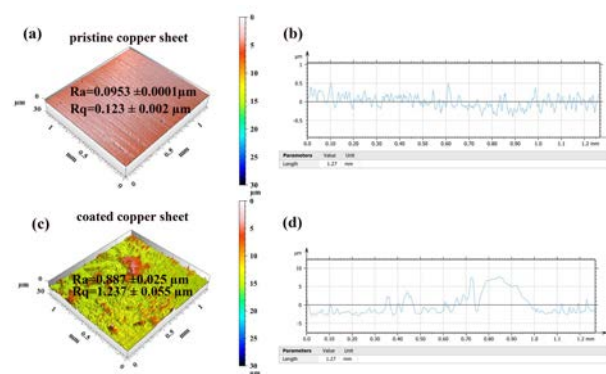


**Figure S17.** The 3D optical microscopic images of the pristine (a, b) and the coated copper sheet (c, d).

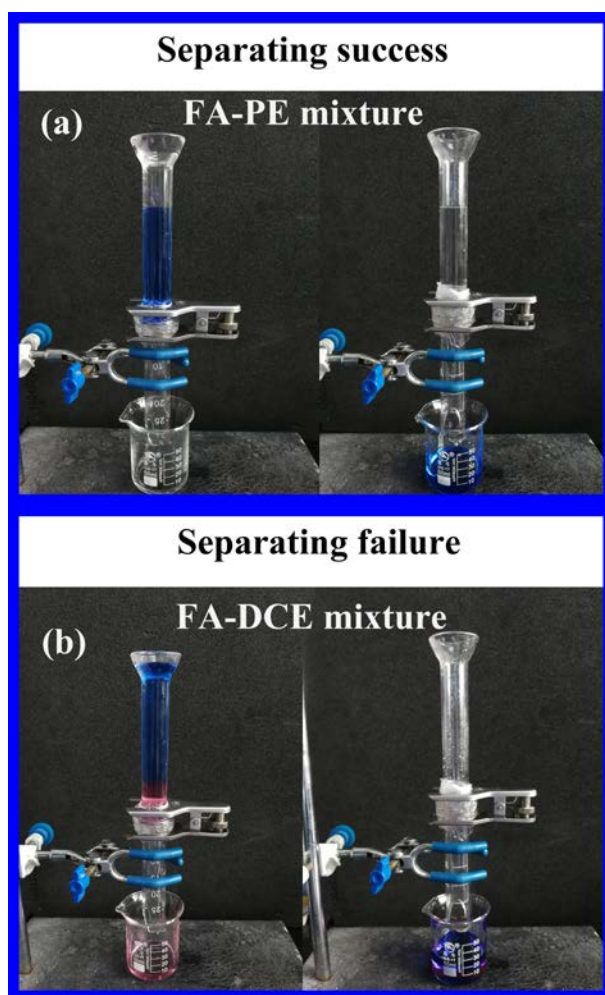


**Figure S18.** The separation photograph of Z(0) SSM in separating FA-PE (a) and FA-DCE mixture (b). The coated SSM only allows high polarity liquids to pass through.

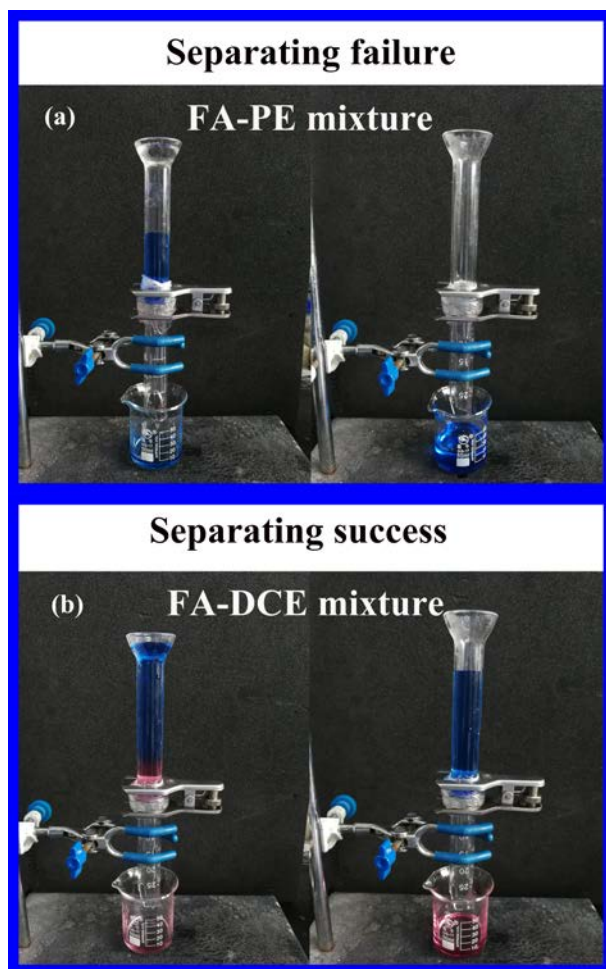


**Figure S19.** The separation photograph of Z(1.0) SSM in separating FA-PE (a) and FA-DCE mixture (b). The coated SSM only allows low polarity liquids to pass through.

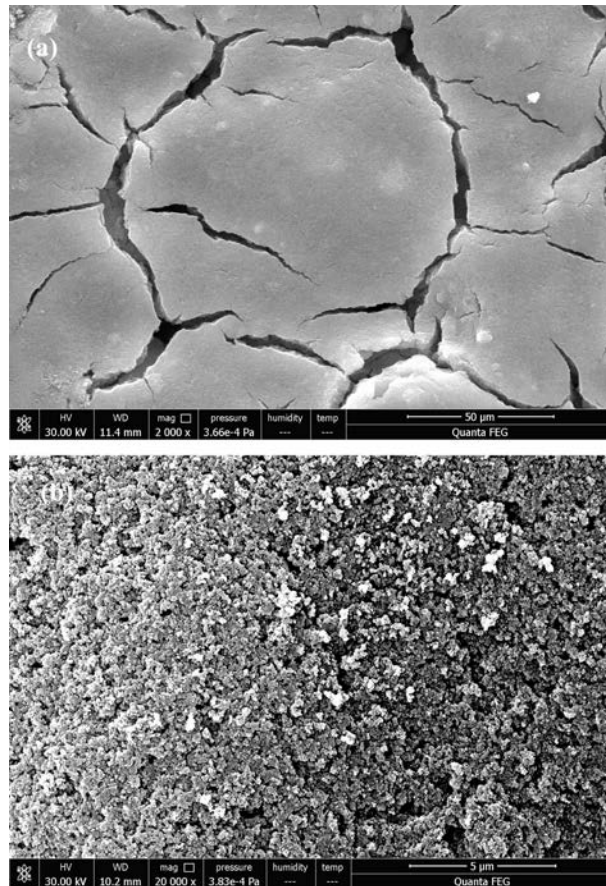


**Figure S20.** The ESEM images of Z(0.1) SSM after 10 on-demand OL separation cycles.

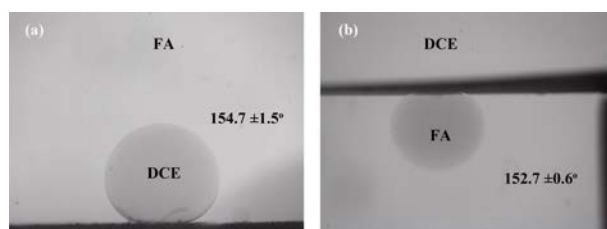


**Figure S21.** The DCE contact angle under FA (a) and FA contact angle under DCE (b) on Z(0.1) SSM after 10 on-demand OL separation cycles.



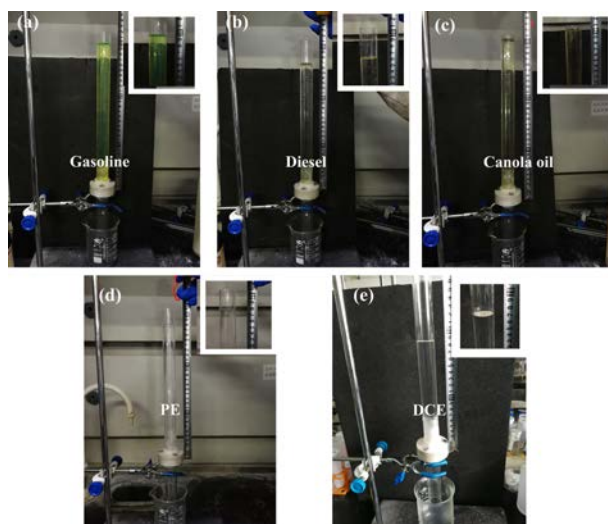


**Figure S22.** The separation photographs of Z(0.1) SSM show the coated mesh exhibits high intrusion pressure for gasoline (a), diesel (b), canola oil (c), PE(d) and DCE(e) when the coated mesh was prewetted by FA.

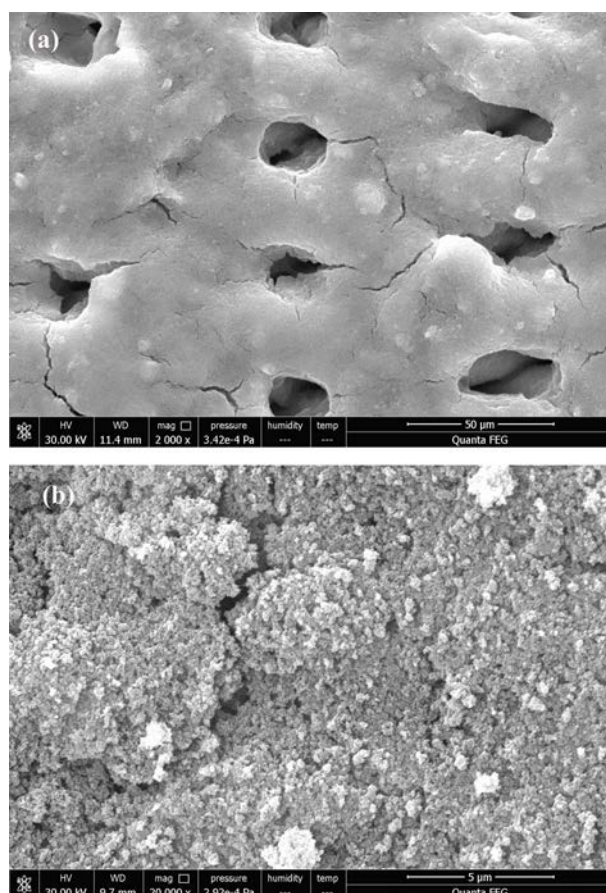


**Figure S23.** ESEM images of Z(0.1) SSM after 5-days 1,2-dichloroethane immersion.

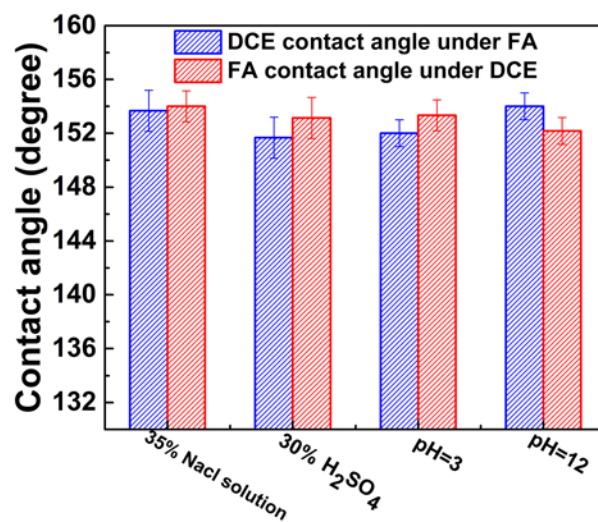


**Figure S24.** The DCE contact angles against FA and FA contact angles against DCE of Z(0.1) SSM after 5-days immersion in various corrosive environment.

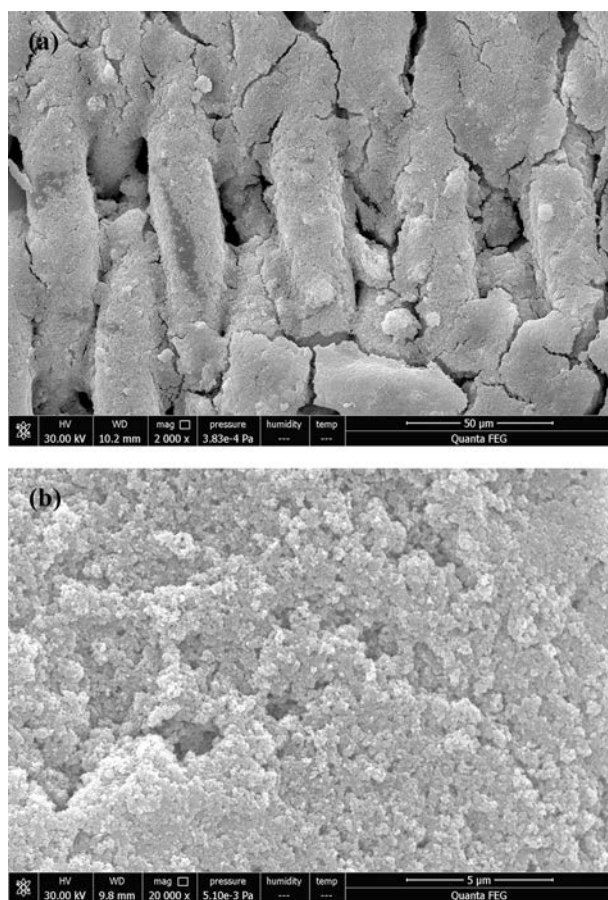


**Figure S25.** ESEM images of Z(0.1) SSM after 5-days 30% H<sub>2</sub>SO<sub>4</sub> immersion.

**Table S1** Organic liquid separation using various superwetting membranes.

Separating membrane	Fabricating method	Separating strategy	On-demand separation?	Separation efficiency	Refs	Scalable fabricating?	Facile fabrication?
SiO <sub>2</sub> -TiO <sub>2</sub> nanofibrous membrane	Electrospinning, calcination, and surface modification	oleophobicity-tunable	No	>99%	1	Yes	No
Cu(OH) <sub>2</sub> Nanoneedles Mesh	Surface oxidation process	oleophobicity-tunable	No	>97%	2	No	No
PVDF-HFP/PFDT MS membranes	Electrospinning	oleophobicity-tunable	No	>97%	3	No	No
SiO <sub>2</sub> -TiO <sub>2</sub> composite porous nanofibrous membranes	Electrospinning	High surface tension liquid-infused and polarity-based protocol	Yes	>99%	4	Yes	No
Copper-coated mesh	Electrodeposition	High surface tension liquid-infused	No	>97%	5	No	Yes
SiO <sub>2</sub> -Capstone FS50 @AP mesh	Spraying coating	Polarity-based protocol	No	>99%	6	No	Yes
Ag/Cu-coated SSM	displacement reaction and galvanostatic method	Polarity-based protocol	Yes	>99%	7	No	No
TiO <sub>2</sub> -Zonyl 9977 coated mesh	Spraying coating	Polarity-based protocol	Yes	>97%	This work	Yes	Yes

**References:**

1. L. Wang, Y. Zhao, Y. Tian and L. Jiang, *Angew. Chem., Int. Ed.*, 2015, **54**, 14732-14737.
2. J. Liu, L. Wang, N. Wang, F. Guo, L. Hou, Y. Chen, J. Liu, Y. Zhao and L. Jiang, *Small*, 2017, **13**, 1600499.

3. L. Hou, L. Wang, N. Wang, F. Guo, J. Liu, Y. Chen, J. Liu, Y. Zhao and L. Jiang, *NPG Asia Mater.*,, 2016, **8**, e334-e334.
4. Y. Wang, J. Di, L. Wang, X. Li, N. Wang, B. Wang, Y. Tian, L. Jiang and J. Yu, *Nat. Commun.*,, 2017, **8**, 575.
5. Z. Zhao, Y. Shen, H. Yang, J. Li and L. Guo, *ACS Appl. Mater. Interfaces*, 2019, **11**, 28370-28376.
6. Y. Sun and Z. Guo, *Chem. Eng. J.*,, 2020, **381**, 122629.
7. L. Tie, J. Li, M. Liu, Z. Guo, Y. Liang and W. Liu, *ACS Appl. Mater. Interfaces*, 2018, **10**, 37634-37642.

**Table S2** The dielectric constant and surface tension of the used liquids at 25 °C.

Liquids	Dielectric constant	Surface tension (mM / m)
Toluene	2.385	30.9
n-Hexadecane	2.046	28.3
1,2-Dichloroethane	12.7	35.43
Diiodomethane	5.316	50.8
Dichloromethane	9.14	30.41
Dimethyl sulfoxide	47.24	43.54
Glycerin	46.5	61.9
Formamide	111	57.45
Water	78.5	72.8
Ethylene glycol	41.4	47.7
Propylene carbonate	69	30

**Table S3** The density of the used liquids at 25 °C.

Liquids	Density (g/m <sup>3</sup> )
petroleum ether (PE)	0.65
Gasoline	0.74
Canola oil	0.909
Diesel	0.84
1,2-dichloroethane (DCE)	1.235